Ablative fractional CO_2 laser treatment promotes wound healing phenotype in skin macrophages

Wiinberg, Martin; Andresen, Thomas L.; Haedersdal, Merete; Olesen, Uffe H.

Published in:
Lasers in Surgery and Medicine

Link to article, DOI:
10.1002/lsm.23772

Publication date:
2024

Document Version
Publisher's PDF, also known as Version of record

Accepted: 13 February 2024

DOI: 10.1002/lsm.23772

PRECLINICAL STUDY

Ablative fractional CO_2 laser treatment promotes wound healing phenotype in skin macrophages

Martin Wiinberg MSc[1] | **Thomas L. Andresen PhD**[1] | **Merete Haedersdal DMSc**[2] | **Uffe H. Olesen PhD**[2]

[1]Department of Health Technology, Technical University of Denmark, Kongens Lyngby, Denmark

[2]Department of Dermatology, Copenhagen University Hospital—Bispebjerg, Copenhagen, Denmark

Correspondence

Martin Wiinberg, MSc, Department of Health Technology, Technical University of Denmark, 2800 Kongens Lyngby, Denmark.
Email: marwii@dtu.dk

Abstract

Objectives: Ablative fractional laser (AFL) treatment is a well-established method for reducing signs of skin photoaging. However, the biological mechanisms underlying AFL-induced healing responses and skin rejuvenation remain largely unknown. It is known that macrophages play an important role in orchestrating healing, normalization, and remodeling processes in skin. Macrophage phenotypes are characterized by inflammatory markers, including arginase-1 (Arg1), major histocompatibility class II molecules (MHC II), and CD206. This study aims to explore AFL's effect on macrophage phenotype by evaluating changes in inflammatory markers and the potential concurrent accumulation of Arg1 in the skin.

Methods: Mice ($n = 9$) received a single AFL treatment on the left side of the back skin (100 mJ/microbeam, 5% density) while the right side of the back remained untreated as control. Treated and untreated skin from each mouse were collected Day 5 posttreatment for flow cytometry and histology analysis. Flow cytometry evaluated the immune infiltration of macrophages and the expression of macrophage inflammatory markers (Arg1, MHC II, and CD206). In addition, Arg1 presence in the skin was evaluated through antibody staining of histology samples and quantification was performed using QuPath image analysis software.

Results: Following AFL, the number of macrophages increased 11-fold ($p = 0.0053$). Phenotype analysis of AFL-treated skin revealed an increase in the percentage of macrophages positive for Arg1 ($p < 0.0001$) and a decrease in the percentage of macrophages positive for MHC II ($p < 0.0001$) compared to untreated skin. No significant differences were observed in percentage of CD206-positive macrophages ($p = 0.8952$). Visualization of AFL-treated skin demonstrated a distinct pattern of Arg1 accumulation that correlated with the microscopic treatment zones (MTZ). Quantification of the percentage of Arg1-positive area in epidermis and dermis showed a significant increase from $3.5\% \pm 1.2\%$ to $5.2\% \pm 1.7$ ($p = 0.0232$) and an increase from $2.2\% \pm 1.2\%$ to $9.6\% \pm 3.3$ ($p < 0.0001$) in whole skin samples.

Conclusion: AFL treatment polarizes macrophages toward a wound healing phenotype and induces Arg1 accumulation in the MTZ. We propose that the polarized wound healing macrophages are a major source for the increased Arg1 levels observed in the skin following treatment.

KEYWORDS

ablative fractional laser, arginase-1, inflammation, macrophages, wound healing

INTRODUCTION

Ablative fractional laser (AFL) is a commonly used noninvasive cosmetic procedure to reduce signs of photoaging.[1–4] The rationale behind using AFL to improve skin appearance is that the controlled thermal microinjury ablates the skin tissue and creates microscopic treatment zones (MTZ), which initiates a healing process that results in improved skin texture and skin tightening, termed skin rejuvenation.[2,5,6] AFL has also been reported to be an effective treatment for reducing scar tissue due to AFL's favorable esthetic outcomes and acceptable adverse effects.[7–9]

Studies of the underlying biological dynamics after AFL treatment of skin have suggested that AFL reinvigorates tissue homeostasis by inducing a wound healing response involving remodeling the extracellular matrix.[6,10] Temporal changes in collagen biosynthesis pathways, matrix metalloproteases, and pro-inflammatory and anti-inflammatory cells and cytokines occur after AFL treatment of skin in a strictly coordinated manner that eventually leads to dermal remodeling.[4,11–14] Macrophages are key players in coordinating this healing process due to their plethora of functions. Every phase in the healing is dominated by different macrophage phenotypes.[15] The early healing phase is dominated by pro-inflammatory macrophages that phagocytose cellular debris and apoptotic neutrophils, while later phases are dominated by anti-inflammatory wound healing macrophages that promote fibroblast migration, angiogenesis, and other processes related to matrix remodeling.[15–17] Previous studies of wound healing responses after skin injury have reported the importance of macrophages in cutaneous wound healing—partly by their secretion of the wound healing promoting enzyme arginase-1 (Arg1).[18] Arg1 is a metabolic enzyme that is involved in the synthesis pathway of L-Proline: one of the components in collagen proteins.[19] Moreover, Arg1 is considered a primary marker of wound healing macrophages that has been shown to inhibit an inflammatory response during wound healing and promote collagen deposition.[15,18,20,21]

While previous studies have indicated that AFL induces infiltration of myeloid immune cells, e.g., macrophages and neutrophil granulocytes in skin,[12,22,23] no studies have investigated AFL's influence on macrophages' phenotype.[12,22,23] In this study, we hypothesize that AFL treatment polarizes skin macrophages toward a wound healing phenotype characterized by an increased level of anti-inflammatory markers (Arg1 and CD206) and decreased major histocompatibility complex class II molecules (MHC II).[15] Thus, this study aims to investigate AFL's impact on the inflammatory phenotype of macrophages in skin characterized by expression of these inflammatory markers. As Arg1 has been shown to be crucial in wound healing, this study examines whether AFL induces concurrent Arg1 accumulation in skin.

MATERIALS AND METHODS

Study design

AFL-treated versus untreated (control) skin was investigated by flow cytometry analysis and immunohistochemical (IHC) analysis. A total of nine mice were included in the study. The back skin of each mouse was divided into a 2 × 2 grid of skin zones measuring 1 cm^2—two zones on the left side of the spine were assigned as the intervention group and two on the right side were assigned as untreated controls. AFL treatment was performed on Day 0. On Day 5, mice were euthanized, and the two upper zones were excised for flow cytometry analysis, and the two lower zones for IHC analysis (Figure 1). The outcome measures were the population of immune cells in skin, including macrophages and neutrophils, macrophage inflammatory markers (MHC II, CD206, and Arg1) analyzed by flow cytometry, and Arg1 protein level in IHC samples of skin.

Animals

Skin samples were collected from immunocompetent transgenic female mice (genotype: *Ptch1*$^{+/-}$) with ages between 16 and 19 weeks.[24] Mice were bred at the University of Copenhagen and housed at Bispebjerg Hospital under controlled conditions (23–24°C temperature at a 12-h daylight cycle with feed and water ad libitum). The study was approved by the Danish Animal Experiments Inspectorate (protocol code 019-15-0201-01666) and conducted in accordance with Directive 2010/63/EU and ARRIVE guidelines. Health monitor screening was performed annually at the facility, according to the Federation of Laboratory Animal Science Association (FELASA), and no pathogens were found in the tests (Idexx BioAnalytics).

Laser intervention

The back hair was trimmed on the day of treatment. Mice were sedated with isoflurane before anesthetized by subcutaneous administration of fentanyl, fluanisone, and midazolam before treatment. Treatment was performed with a single exposure of ablative fractional 10,600 nm CO_2-laser (100 mJ/microbeam, 5% density) from an Ultrapulse® instrument with DeepFx handpiece (Lumenis, Inc.). The laser settings were chosen to induce full-thickness penetration and thereby, ensure a robust biological response in all skin layers. A study in pigs have shown that 80 mJ/microbeam results in a 1328 μm penetration depth.[25] From histology samples, the skin thickness of our model (epidermis, dermis, and hypodermis) is estimated to be approximately 800–1100 μm (Supporting Information: Figure S3). Histological evaluation of skin samples verified

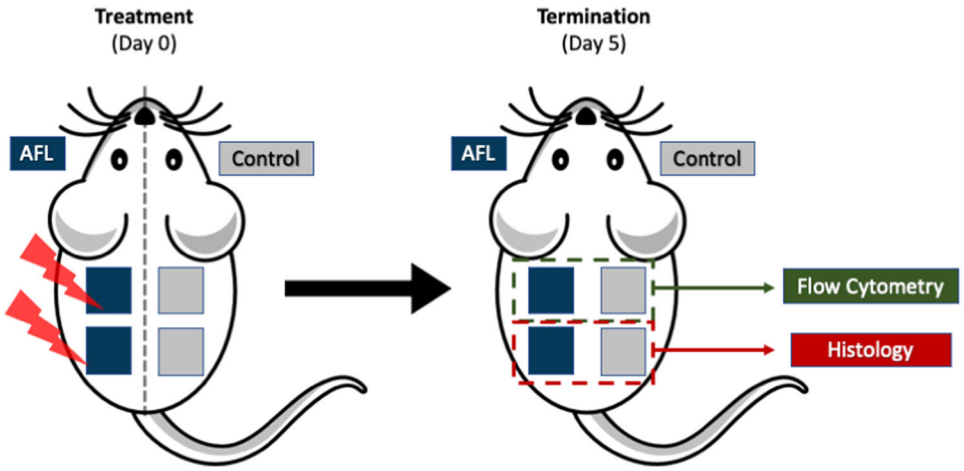

FIGURE 1 Study design: Two 1 cm^2 skin zones on left side of the spine were treated with AFL (100 mJ/microbeam, 5% density) on Day 0, and the right side was left untreated. At termination on Day 5, the upper pair of zones were excised for flow cytometry and the lower pair for histology.

full-thickness penetration of the AFL treatment (Supporting Information: Figure S3).

Flow cytometry

The skin samples were fragmented and digested in Mouse Tumor Dissociation Kit (Miltenyi Biotec, cat#130-096-730) at 37°C for 1 h in Precision SWB 27 Shaking Water Bath (Thermo Fisher Scientific, cat# TSSWB27, RRID: SCR_020738). Cell suspensions were passed through 70 µm cell strainers. Total cell numbers were measured using Guava Muse Cell Analyzer (Luminex, RRID:SCR_020252) according to the manufacturer's guidelines. Samples were stained in a 96-well and washed in FACS buffer (0.5% bovine serum albumin [BSA] and 0.1% sodium azide in phosphate-buffered saline [PBS]). Fc receptors were blocked by resuspending samples in 50 µg/ml purified anti-mouse CD16/CD32 (BD Biosciences, cat#553142, RRID:AB_394657) and incubated on ice for 5 min. Cells were then incubated with antibodies and viability dye (Supporting Information: Table S1) for 30 min on ice protected from light. Following surface staining, a total of three washed in FACS buffer and resuspended in fixation buffer for 60 min. (eBioscience, cat#00-5523-00). To intracellular stain cells for Arg1, cells were washed in permeabilization buffer (eBioscience, cat#00-5523-00) then Fc blocked before subsequently intracellular staining. Samples were washed three times in permeabilization buffer and filtered through a 70 µm cell strainer before acquisition the following day on LSRFortessa X-20 Fortessa Flow Cytometer (BD Biosciences, RRID:SCR_019600). Single-color stained UltraComp eBeads™ Plus Compensation Beads (Invitrogen, cat# 01-3333) were used to compensate for spectral spillover. All flow cytometry data were analyzed using FlowJo v10.7 (FlowJo LCC, https://www.flowjo.com/, RRID:SCR_008520). Immune cells were gated as viability dye^-, $CD45^+$ cells. Neutrophils were defined as immune cells that were $CD11b^+$ and $Ly6G^+$, $F4/80^-$. Macrophages were defined as immune cells that were $CD11b^+$ and $Ly6G^-$, $F4/80^+$. The gating strategy is provided in Supporting Information: Figure S1. Fluorescence intensities from flow cytometry were reported as geometric mean fluorescence intensity, henceforth named signal intensity. Total cells of cell type per milligram tissue was determined as: ("Cell type frequency of scatter" × "Total cell numbers")/Total weight of sample. Cell type frequency is provided in Supporting Information: Figure S2.

Immunohistochemistry

Skin samples were fixated in 4% formalin buffer and processed using Shandon™ Excelsior ES® (Thermo Fisher Scientific), in which tissue was embedded in paraffin. Samples were sectioned at 3 µm using Shandon Finesse Series Microtome (Thermo Fisher Scientific). Sections were deparaffinized, rehydrated, and antigen-retrieval was performed with citrate buffer at pH 6.0 and 600 W effect 3 × 5 min in Miele Supratonic M 705 microwave. Sections were blocked with 10% goat serum in TBS buffer for 20 min and stained with 0.4 µg/mL primary rabbit anti-mouse Arg1 antibody (Thermo Fisher Scientific, cat#PA5-29645, RRID:AB_2547120) in incubation buffer (1% BSA in TBS buffer) for 1 h at room temperature. Sections incubated with 2.0 µg/mL goat anti-rabbit IgG HRP secondary antibody (Abcam, cat#ab205718, RRID:AB_2819160) for 1 h at room temperature before incubation with DAB substrate (Abcam, cat#ab64238) for 7 min. Sections were counterstained with hematoxylin and mounted on a microscope slide with Pertex® Mounting Medium (Histolab, cat#00811). Stained slides were scanned with MoticEasyScan Pro (Motic, RRID:SCR_022814) at a ×40 magnitude. QuPath Software [26] v0.3.2 (https://qupath.github.io/) was

used to quantify the relative Arg1 protein level (measured as positive DAB stain) in skin samples. Samples were manually segmented to select the area of interest (either epidermis and dermis or whole skin sample) before further segmenting by thresholding. The percentage of Arg1-positive area within the area of interest was measured by thresholding. See Supporting Information: Table S2 parameters for segmentation and Arg1 measurement.

Visualization and statistics

Statistical testing was performed using a two-tailed paired Student-*t*-test. Prism 9 (GraphPad Software, https://www.graphpad.com/) was used for data visualization and statistical analysis. The significance level was set to $\alpha = 0.05$ for all statistical testing. Flow cytometry and IHC outcome assessment and data analysis were performed blinded, and unblinding happened after data analysis. Numbers in text are reported as mean ± standard deviation.

RESULTS

AFL leads to increased number of macrophages in skin

The number of immune cells per milligram skin tissue was significantly increased after AFL treatment from 57 ± 21.0 in control group to 1027 ± 628.3 in AFL group ($p = 0.0016$, Figure 2A). Further analysis of the immune cells revealed an approximately 11-fold increase in the number of macrophages per milligram tissue from 5 ± 2.6 in control group to 56 ± 40.6 in the AFL group ($p = 0.0053$, Figure 2B). Additionally, AFL treated skin had a pronounced neutrophil infiltration with an increase in neutrophils per milligram tissue from 2 ± 1.0 in control group to 272 ± 230.4 in AFL group ($p = 0.0078$, Figure 2C). Various degrees of ulceration were observed in 8 out of 18 AFL-treated skin samples; however, no significant differences were observed between ulcerated and non-ulcerated skin with regard to immune infiltration or other measured outcomes (Supporting Information: Table S3).

Increased Arg1 and lower MHC II levels in macrophages

The percentage of Arg1-positive macrophages was significantly increased in AFL group ($p < 0.0001$, Figure 3A) and the signal intensity of Arg1 in macrophages was higher in AFL group compared to in control group ($p = 0.0004$), meaning that each macrophage had more Arg1 expressed on average in AFL group than in control group (Figure 3B). The percentage of macrophages expressing MHC II was significantly lower in the AFL group compared to control group ($p < 0.0001$, Figure 3C) and the signal intensity of MHC II was lower on macrophages in AFL-treated skin than control skin ($p < 0.0001$, Figure 3D). No significant difference was observed in the percentage of macrophages expressing the anti-inflammatory marker, CD206 ($p = 0.8952$), or in the signal intensity of CD206 ($p = 0.7267$, Figure 3E,F). On neutrophils, both the percentage and the signal intensity of MHC II molecules were reduced in AFL group compared to control group ($p = 0.0004$, $p < 0.0001$) (Figure 3G,H). However, the signal intensity values indicate that the expression of MHC II on neutrophils is minimal compared with macrophages. Both CD206 and Arg1 levels in neutrophils were too low to be detected.

Accumulation of Arg1 protein in microscopic treatment zones in the skin

Examination of IHC slides showed elevated Arg1 protein levels concentrated in distinct columnar pattern across the AFL-treated skin samples (Figure 4A,B). The locations of the Arg1 positive columns approximately correlated with

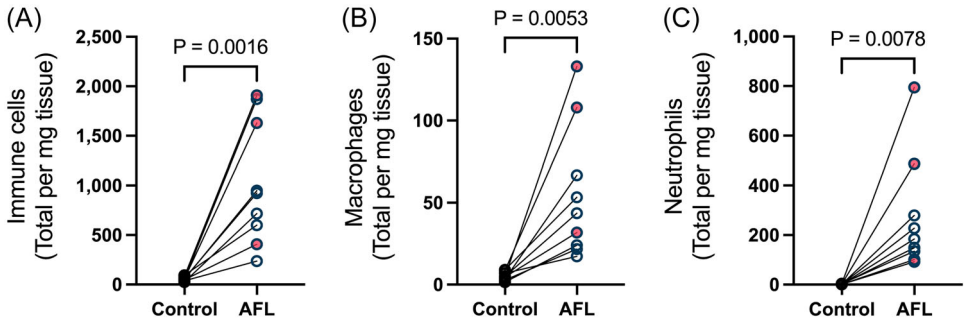

FIGURE 2 Flow cytometry analysis of immune cells in skin shows increased immune infiltration of neutrophils and macrophages after ablative fractional laser (AFL) treatment. Number of immune cells per milligram tissue (A). Similar for macrophages (B) and neutrophils (C). The lines on the plots connect the control and AFL sample pair from each mouse. Red circles indicate ulceration of the skin on the day of termination. Immune cells were gated as $CD45^+$, neutrophils as $CD45^+CD11b^+Ly6G^+F4/80^-$ and macrophages as $CD45^+CD11b^+Ly6G^-F4/80^+$. Sample size $n = 9$ per group. Two-tailed paired *t*-test was used for statistical testing.

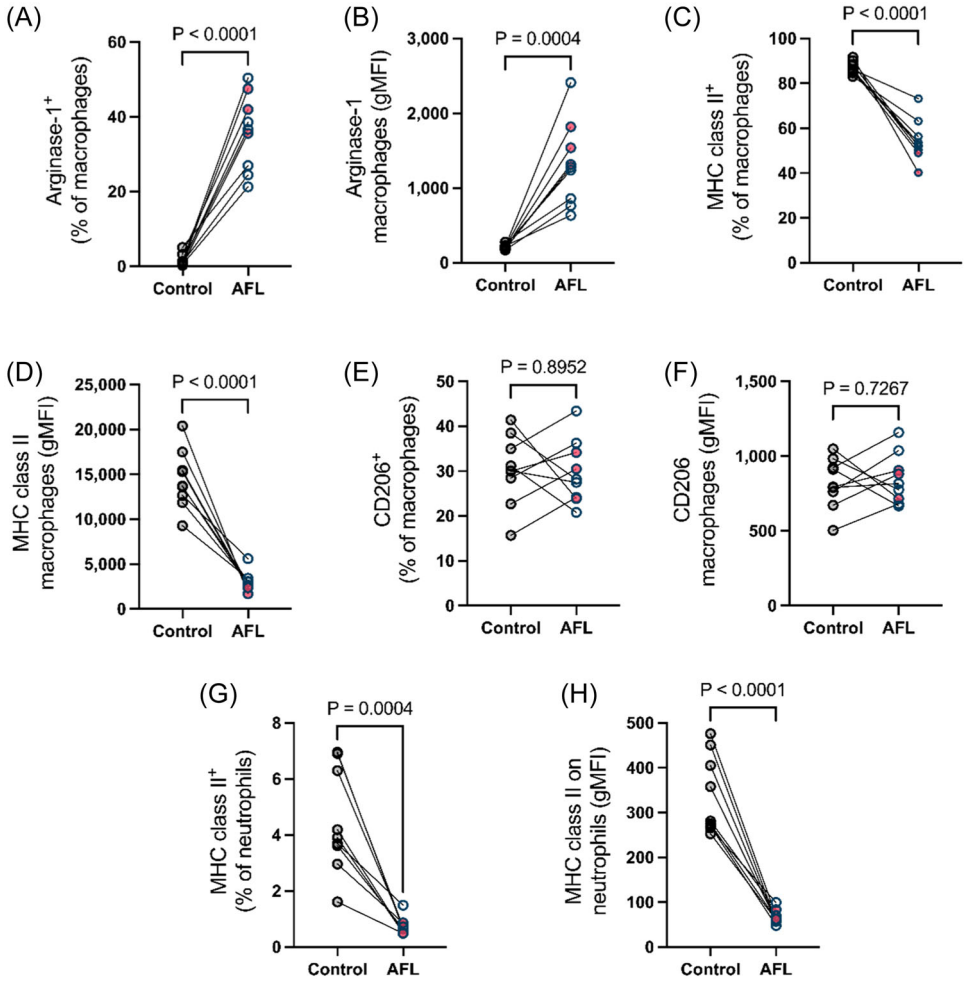

FIGURE 3 Phenotype analysis shows elevated arginase-1 levels and lower major histocompatibility complex class II molecules (MHC II) on macrophages. Percentage of macrophages positive for Arg1 (A) and signal intensity (gMFI) of Arg1 in macrophages (B). Similar parameters for MHC II surface marker expression (C–D) and CD206 expression on macrophages (E–F). MHC II on neutrophils, both percentage positive neutrophils (G) and signal intensity of MHC II (H). The lines on the plots connect the control and ablative fractional laser (AFL) sample pair from each mouse. Red circles indicate ulceration of the skin on the day of termination. Sample size of $n = 9$ per group. Two-tailed paired *t*-test was used for statistical testing.

the location of the microscopic treatment zones (MTZ) (Supporting Information: Figure S4). Arg1 was both present in the epidermal layer and through dermis, though Arg1 was even more prominent deeper into the hypodermis and the underlying connective tissue layer (Figure 4A,B). Quantification of Arg1-positive area in the epidermis and dermis showed a higher Arg1 protein level in AFL-treated skin (5.2% ± 1.7%) than in control skin (3.5% ± 1.2%) ($p = 0.0232$, Figure 4C). Further, the Arg1-positive area in the whole sample was increased in AFL-treated skin (9.6% ± 3.3%) compared with the control skin (2.2% ± 1.2%, $p < 0.0001$, Figure 4D).

DISCUSSION

The cellular and molecular factors involved in the skin healing response after AFL are highly complex and are yet to be fully understood. Previous studies of AFL have reported to stimulate numerous cell types and factors that are involved in the cutaneous remodeling and healing process.[11,12,22] However, to our knowledge, this study is the first to show that AFL induces a significant increase in Arg1 production by macrophages and that AFL results in an accumulation of Arg1 in the MTZ. These findings suggest that AFL polarizes the phenotype of the skin macrophage toward a wound healing phenotype which is supported by the observed decrease in the expression of the pro-inflammatory marker, MHC II. Previous studies have shown that AFL increases *TGF-β* mRNA expression.[12] TGF-β is a potent stimulator of wound healing as it stimulates collagen I and III production in fibroblasts,[27–29] and interestingly, TGF-β has also been shown to polarize macrophages toward a wound healing phenotype[30] and induce expression of Arg1 in macrophages in vitro.[31]

Three primary markers of macrophage inflammatory phenotype were evaluated in the study: Arg1, MHC II

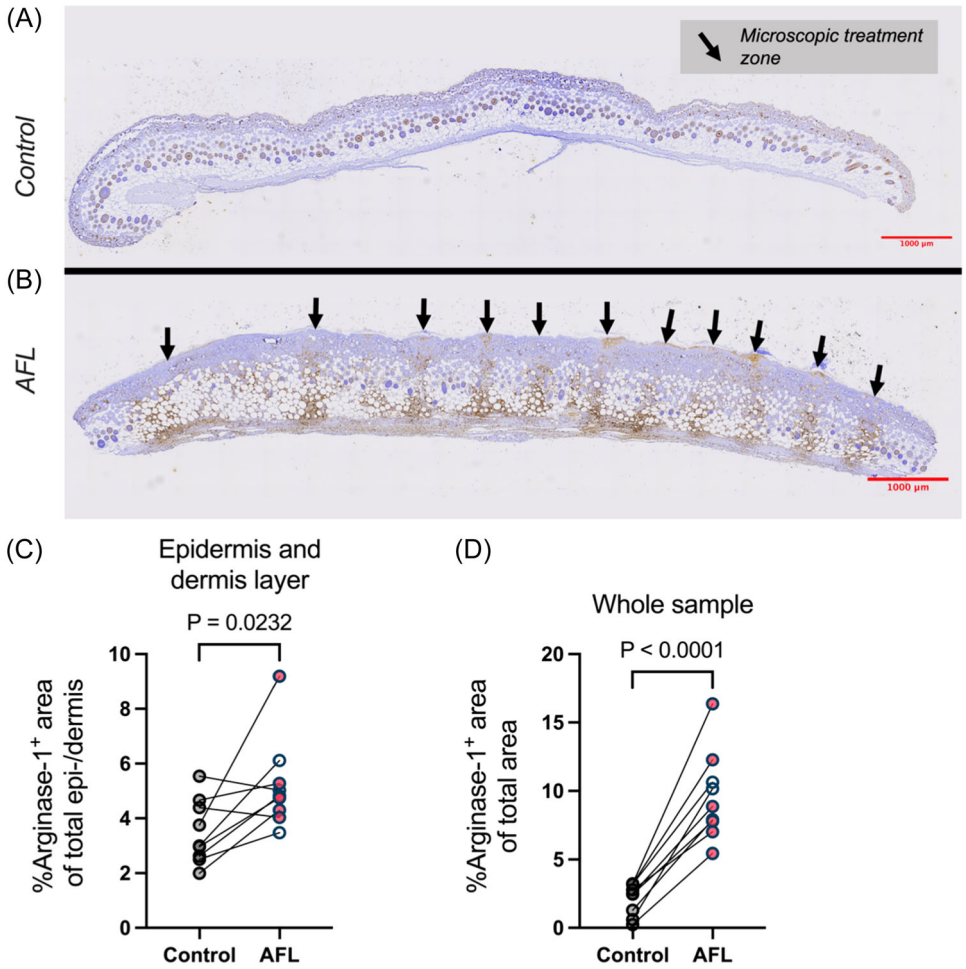

FIGURE 4 Immunohistochemical analysis reveals arginase-1 protein accumulation in microscopic treatment zones caused by ablative fractional laser (AFL) treatment: Digitalized microscopy images of arginase-1 stained immunohistochemical slides of control skin (A) and AFL skin (B). Percentage of $Arg1^+$ area out of all tissue area in epidermis and dermis layer (C) and in the whole skin sample (D). Arrows specify microscopic treatment zones. The lines on the plots connect the control and AFL sample pair from each mouse. Red circles indicate ulceration of the skin on the day of termination. Sample size of $n = 9$ per group. Two-tailed paired *t*-test was used for statistical testing.

and CD206. Arg1 is considered an anti-inflammatory protein as it suppresses cytotoxic T-cell responses.[20,32,33] CD206 is also an anti-inflammatory marker observed in certain populations of wound healing macrophages.[15,20] Conversely, MHC II is considered pro-inflammatory due to its involvement in antigen-presentation[34] and MHC II would be expected to be decreased in macrophages with a wound healing phenotype. In response to AFL, results showed that Arg1 was increased, and MHC II decreased in macrophages, but no differences were observed in the percentage of CD206-positive macrophages after treatment in our study. This observation is unexpected as CD206 has previously been reported to be upregulated in murine skin at day 7 after thermal induced injury.[35] Overall, the increase in Arg1-positive macrophages and downregulation of MHC II positive macrophages implies that AFL provokes a shift in macrophage populations toward an anti-inflammatory, wound healing phenotype, particularly due to the notable upregulation of Arg1.

In the current study, macrophages in AFL-treated skin showed a high level of Arg1 protein expression. In addition, Arg1 was found to accumulate in MTZs. Even though this study does not demonstrate a direct causal relationship between Arg1-producing macrophages and the accumulation of Arg1 in skin tissue, we hypothesize that the macrophages are a major cellular source of observed Arg1 accumulation in the skin. This result is consistent with a previous finding in a study by Campbell et al.[18] They report that Arg1 is dynamically regulated during acute cutaneous wound healing with a peak Arg1 concentration in the skin at day 5 after injury. Campbell et al. proposes that Arg1 production by macrophages is crucial for optimal healing after injury and is involved in the re-epithelization of the wounded area. They demonstrate that the lack of Arg1 during cutaneous healing reduced collagen deposition and delayed wound healing. However, macrophages are not necessarily the only cell type involved in Arg1 production in response to injury. A recent study by the same group of researchers showed

that keratinocytes also express Arg1 upon cutaneous injury, and depletion of Arg1 genes in epidermal keratinocytes results in delayed cutaneous wound healing.[36] Nevertheless, our findings suggest AFL induces Arg1-expressing wound healing macrophages in the skin. This can contribute to the healing response and potentially facilitate skin rejuvenation, as Arg1 expression correlates to collagen deposition.[19,37] Whether macrophages are the main source of the accumulated Arg1 and whether Arg1 results in collagen deposition in MTZs and the surrounding skin tissue and thereby, facilitates dermal remodeling of photoaged skin is yet to be investigated.

Neutrophils are the first immune cell responders to tissue injury. Here, neutrophils phagocytose cellular debris and support tissue repair through the secretion of wound healing factors, for example, growth factors and matrix-degrading enzymes. We found that AFL treatment induced a pronounced neutrophil infiltration in the skin which may have a negative impact on the healing response, as a previous study found that excessive neutrophil infiltration and inflammation of the skin resulted in an impaired wound healing response in mice.[12] In the current study, histology samples showed a full skin microbeam penetration, and we observed various degrees of ulceration in 8 out of 18 treated zones. In a clinical setting, we would advocate for a considerably lower energy level of the AFL to substantially decrease the risk of ulceration.

While this study demonstrates that AFL treatment promotes wound healing phenotype in macrophages and induces Arg1 accumulation in skin, it is important to recognize that these findings are limited to a single time point. Additional time points, both earlier than Day 5 and during later phases of wound healing, are required to further elucidate temporal dynamics of macrophage phenotype and kinetics of Arg1. The next step involves exploring whether Arg1 is a prerequisite for the clinically observed AFL-induced dermal remodeling effects. In relation to this, it would be interesting to quantify AFL effects on extracellular matrix proteins such as collagen type I and matrix metalloproteases if Arg1 activity was inhibited. Lastly, it is relevant to examine how laser energy exposure correlates with Arg1 protein and wound healing macrophage phenotype in a clinical study as the optimal energy levels in a clinical context would typically be lower than those applied in this study. We hypothesize that reducing AFL energy would result in similar macrophage polarization and Arg1 induction, although the impact may be less pronounced than in the present study.

CONCLUSION

In summary, AFL treatment resulted in an increased population of skin macrophages that were of anti-inflammatory wound healing phenotype with high Arg1 protein expression indicating a healing response. The AFL intervention group had significant cutaneous accumulation in Arg1 in a pattern resembling the MTZs following AFL treatment. Collectively, the results show that AFL induces Arg1 accumulation in skin and the results imply that the AFL-promoted wound healing macrophages are possibly a major source of the increased Arg1 levels observed in the skin after treatment. Overall, this study provides novel insights into the cutaneous biological response to AFL therapy that can help uncover the underlying mechanisms of AFL-induced skin rejuvenation.

ACKNOWLEDGMENTS

The authors would like to thank Susanne Primdahl from the Technical University of Denmark and Diana Høeg from Copenhagen University Hospital for their technical assistance in producing and staining histology and immunohistochemical samples. The work was supported by the Independent Research Fund Denmark—Medical Sciences (DFF-FSS) grant number 1030-00232B and Greater Copenhagen Health Science Partners (GCHSP). The research was executed as part of Skin Cancer Innovation Clinical Academic Group (SCIN-CAG) of Greater Copenhagen Health Science Partners and the Danish Research Center for Skin Cancer (www.researchcenterforskincancer.org), a public-private research partnership between the Private Hospital Molholm, Aalborg University Hospital and Copenhagen University Hospital, Bispebjerg.

CONFLICT OF INTEREST STATEMENT

The authors declare no conflict of interest.

ORCID

Martin Wiinberg http://orcid.org/0000-0001-6999-0557
Thomas L. Andresen http://orcid.org/0000-0002-1048-127X
Merete Haedersdal http://orcid.org/0000-0003-1250-2035
Uffe H. Olesen http://orcid.org/0000-0002-4578-684X

REFERENCES

1. Anderson RR. Lasers for dermatology and skin biology. J Invest Dermatol. 2013;133:E21–3. https://doi.org/10.1038/skinbio.2013.181
2. Kohl E, Meierhöfer J, Koller M, Zeman F, Klein A, Hohenleutner U, et al. Fractional carbon dioxide laser resurfacing of rhytides and photoageing: a prospective study using profilometric analysis. Br J Dermatol. 2014;170(4):858–65. https://doi.org/10.1111/bjd.12807
3. Tierney EP, Hanke WD, Petersen J, Bartley T, Eckert JR, McCutchen C. Clinical and echographic analysis of ablative fractionated carbon dioxide laser in the treatment of photodamaged facial skin. Dermatol Surg. 2010;36(12):2009–21. https://doi.org/10.1111/j.1524-4725.2010.01766.x
4. Garza LA, Sheu M, Kim N, Tsai J, Alessi Cesar SS, Lee J, et al. Association of early clinical response to laser rejuvenation of photoaged skin with increased lipid metabolism and restoration of skin barrier function. J Invest Dermatol. 2023;143:374–385.e7. https://doi.org/10.1016/j.jid.2022.07.024

5. Park SH, Kim DW, Jeong T. Skin-tightening effect of fractional lasers: comparison of non-ablative and ablative fractional lasers in animal models. J Plast Reconstr Aesthet Surg. 2012;65(10):1305–11. https://doi.org/10.1016/j.bjps.2012.04.028
6. Grunewald S, Bodendorf M, Illes M, Kendler M, Simon JC, Paasch U. In vivo wound healing and dermal matrix remodelling in response to fractional CO_2 laser intervention: clinico-pathological correlation in non-facial skin. Int J Hyperthermia. 2011;27(8):811–8. https://doi.org/10.3109/02656736.2011.595380
7. Seago M, Shumaker PR, Spring LK, Alam M, Al-Niaimi F, Rox Anderson R, et al. Laser treatment of traumatic scars and contractures: 2020 international consensus recommendations. Lasers Surg Med. 2020;52(2):96–116. https://doi.org/10.1002/LSM.23201
8. Hunzeker CM, Weiss ET, Geronemus RG. Fractionated CO_2 laser resurfacing: our experience with more than 2000 treatments. Aesthet Surg J. 2009;29(4):317–22. https://doi.org/10.1016/j.asj.2009.05.004
9. Hedelund L, Haak CS, Togsverd-Bo K, Bogh MK, Bjerring P, Hædersdal M. Fractional CO_2 laser resurfacing for atrophic acne scars: a randomized controlled trial with blinded response evaluation. Lasers Surg Med. 2012;44(6):447–52. https://doi.org/10.1002/lsm.22048
10. Helbig D, Paasch U. Molecular changes during skin aging and wound healing after fractional ablative photothermolysis. Skin Res Technol. 2011;17(1):119–28. https://doi.org/10.1111/J.1600-0846.2010.00477.X
11. Sherrill JD, Finlay D, Binder RL, Robinson MK, Wei X, Tiesman JP, et al. Transcriptomic analysis of human skin wound healing and rejuvenation following ablative fractional laser treatment. PloS one. 2021;16(11 November):e0260095. https://doi.org/10.1371/JOURNAL.PONE.0260095
12. Zheng W, Zhu Z, Shi Y, Wen S, Ye L, Man M, et al. Neutrophils and their extracellular traps impair ablative fractional carbon dioxide laser-induced dermal remolding in mice. Lasers Surg Med. 2022;54(5):779–89. https://doi.org/10.1002/LSM.23526
13. Qu L, Liu A, Zhou L, He C, Grossman PH, Moy RL, et al. Clinical and molecular effects on mature burn scars after treatment with a fractional CO_2 laser. Lasers Surg Med. 2012;44(7):517–24. https://doi.org/10.1002/LSM.22055
14. DeBruler DM, Blackstone BN, Baumann ME, McFarland KL, Wulff BC, Wilgus TA, et al. Inflammatory responses, matrix remodeling, and re-epithelialization after fractional CO_2 laser treatment of scars. Lasers Surg Med. 2017;49(7):675–85. https://doi.org/10.1002/LSM.22666
15. Krzyszczyk P, Schloss R, Palmer A, Berthiaume F. The role of macrophages in acute and chronic wound healing and interventions to promote pro-wound healing phenotypes. Front Physiol. 2018;9(MAY):419. https://doi.org/10.3389/FPHYS.2018.00419
16. Hesketh M, Sahin KB, West ZE, Murray RZ. Macrophage phenotypes regulate scar formation and chronic wound healing. Int J Mol Sci. 2017;18(7):1545. https://doi.org/10.3390/IJMS18071545
17. Li M, Hou Q, Zhong L, Zhao Y, Fu X. Macrophage related chronic inflammation in non-healing wounds. Front Immunol. 2021;12:12. https://doi.org/10.3389/fimmu.2021.681710
18. Campbell L, Saville CR, Murray PJ, Cruickshank SM, Hardman MJ. Local arginase 1 activity is required for cutaneous wound healing. J Invest Dermatol. 2013;133(10):2461–70. https://doi.org/10.1038/jid.2013.164
19. Szondi DC, Wong JK, Vardy LA, Cruickshank SM. Arginase signalling as a key player in chronic wound pathophysiology and healing. Front Mol Biosci. 2021;8:1049. https://doi.org/10.3389/FMOLB.2021.773866
20. Daley JM, Brancato SK, Thomay AA, Reichner JS, Albina JE. The phenotype of murine wound macrophages. J Leukoc Biol. 2009;87(1):59–67. https://doi.org/10.1189/jlb.0409236
21. Munder M, Eichmann K, Morán M, Centeno F, Soler G, Modolell M. Th1/Th2-regulated expression of arginase isoforms in murine macrophages and dendritic cells. J Immunol. 1999;163(7):3771–7. https://doi.org/10.4049/JIMMUNOL.163.7.3771
22. Helbig D, Bodendorf MO, Grunewald S, Kendler M, Simon JC, Paasch U. Immunohistochemical investigation of wound healing in response to fractional photothermolysis. J Biomed Opt. 2009;14(6):064044. https://doi.org/10.1117/1.3275479
23. Hasegawa K, Fujimoto T, Mita C, Furumoto H, Inoue M, Ikegami K, et al. Single-cell transcriptome analysis of fractional CO_2 laser efficiency in treating a mouse model of alopecia. Lasers Surg Med. 2022;54(8):1167–76. https://doi.org/10.1002/LSM.23590
24. So PL, Lee K, Hebert J, Walker P, Lu Y, Hwang J, et al. Topical tazarotene chemoprevention reduces basal cell carcinoma number and size inPtch1+/− mice exposed to ultraviolet or ionizing radiation. Cancer Res. 2004;64(13):4385–9. https://doi.org/10.1158/0008-5472.CAN-03-1927
25. Olesen UH, Clergeaud G, Hendel KK, Yeung K, Lerche CM, Andresen TL, et al. Enhanced and sustained cutaneous delivery of vismodegib by ablative fractional laser and microemulsion formulation. J Invest Dermatol. 2020;140(10):2051–9. https://doi.org/10.1016/j.jid.2020.01.032
26. Bankhead P, Loughrey MB, Fernández JA, Dombrowski Y, McArt DG, Dunne PD, et al. QuPath: open source software for digital pathology image analysis. Sci Rep. 2017;7(1):16878. https://doi.org/10.1038/S41598-017-17204-5
27. Varga J, Rosenbloom J, Jimenez SA. Transforming growth factor β (TGFβ) causes a persistent increase in steady-state amounts of type I and type III collagen and fibronectin mRNAs in normal human dermal fibroblasts. Biochem J. 1987;247(3):597–604. https://doi.org/10.1042/BJ2470597
28. Abraham DJ, Shiwen X, Black CM, Sa S, Xu Y, Leask A. Tumor necrosis factor α suppresses the induction of connective tissue growth factor by transforming growth factor-β in normal and scleroderma fibroblasts. J Biol Chem. 2000;275(20):15220–5. https://doi.org/10.1074/JBC.275.20.15220
29. Roberts AB, Sporn MB, Assoian RK, Smith JM, Roche NS, Wakefield LM, et al. Transforming growth factor type beta: rapid induction of fibrosis and angiogenesis in vivo and stimulation of collagen formation in vitro. Proc Natl Acad Sci U S A. 1986;83(12):4167–71. https://doi.org/10.1073/PNAS.83.12.4167
30. Gong D, Shi W, Yi S, Chen H, Groffen J, Heisterkamp N. TGFβ signaling plays a critical role in promoting alternative macrophage activation. BMC Immunol. 2012;13:31. https://doi.org/10.1186/1471-2172-13-31
31. Boutard V, Havouis R, Fouqueray B, Philippe C, Moulinoux JP, Baud L. Transforming growth factor-beta stimulates arginase activity in macrophages. implications for the regulation of macrophage cytotoxicity. J Immunol. 1995;155(4):2077–84. https://doi.org/10.4049/jimmunol.155.4.2077
32. Kung JT, Brooks SB, Jakway JP, Leonard LL, Talmage DW. Suppression of in vitro cytotoxic response by macrophages due to induced arginase. J Exp Med. 1977;146(3):665–72. https://doi.org/10.1084/JEM.146.3.665
33. Martí i Líndez AA, Reith W. Arginine-dependent immune responses. Cell Mol Life Sci. 2021;78(13):5303–24. https://doi.org/10.1007/S00018-021-03828-4.
34. Buxadé M, Huerga Encabo H, Riera-Borrull M, Quintana-Gallardo L, López-Cotarelo P, Tellechea M, et al. Macrophage-specific MHCII expression is regulated by a remote Ciita enhancer controlled by NFAT5. J Exp Med. 2018;215(11):2901–18. https://doi.org/10.1084/jem.20180314

35. Pi L, Fang B, Meng X, Qian L. LncRNA XIST accelerates burn wound healing by promoting M2 macrophage polarization through targeting IL-33 via miR-19b. Cell Death Discov. 2022;8(1):220. https://doi.org/10.1038/s41420-022-00990-x
36. Crompton RA, Williams H, Campbell L, Hui Kheng L, Saville C, Ansell DM, et al. An epidermal-specific role for Arginase1 during cutaneous wound repair. J Invest Dermatol. 2022;142(4):1206–16. https://doi.org/10.1016/j.jid.2021.09.009
37. Durante W, Liao L, Reyna SV, Peyton KJ, Schafer AI. Transforming growth factor-1 stimulates L-arginine transport and metabolism in vascular smooth muscle cells role in polyamine and collagen synthesis. Circulation. 2001;103:1121–7. https://doi.org/10.1161/01.cir.103.8.1121

SUPPORTING INFORMATION

Additional supporting information can be found online in the Supporting Information section at the end of this article.

How to cite this article: Wiinberg M, Andresen TL, Haedersdal M, Olesen UH. Ablative fractional CO_2 laser treatment promotes wound healing phenotype in skin macrophages. Lasers Surg Med. 2024;56:270–8. https://doi.org/10.1002/lsm.23772